

Generating Signals with Multiscale Time Irreversibility: The Asymmetric Weierstrass Function

ANTON BURYKIN,^{1*} MADALENA D. COSTA,^{2,3} CHUNG-KANG PENG,² ARY L. GOLDBERGER^{2,3}
AND TIMOTHY G. BUCHMAN¹

¹Emory Center for Critical Care (ECCC) and Department of Surgery, Emory University School of Medicine, Atlanta, GA; ²Margret and H.A. Rey Institute of Nonlinear Dynamics in Physiology and Medicine, Division of Interdisciplinary Medicine and Biotechnology, Beth Israel Deaconess Medical Center, Harvard Medical School, Boston, MA; and ³Wyss Institute for Biologically Inspired Engineering at Harvard University

Received June 16, 2010; accepted June 16, 2010

Time irreversibility (asymmetry with respect to time reversal) is an important property of many time series derived from processes in nature. Some time series (e.g., healthy heart rate dynamics) demonstrate even more complex, multiscale irreversibility, such that not only the original but also coarse-grained time series are asymmetric over a wide range of scales. Several indices to quantify multiscale asymmetry have been introduced. However, there has been no simple generator of model time series with "tunable" multiscale asymmetry to test such indices. We introduce an asymmetric Weierstrass function W_A (constructed from asymmetric sawtooth functions instead of cosine waves) that can be used to construct time series with any given value of the multiscale asymmetry. We show that multiscale asymmetry appears to be independent of other multiscale complexity indices, such as fractal dimension and multiscale entropy. We further generalize the concept of multiscale asymmetry by introducing time-dependent (local) multiscale asymmetry and provide examples of such time series. The W_A function combines two essential features of complex fluctuations, namely fractality (self-similarity) and irreversibility (multiscale time asymmetry); moreover, each of these features can be tuned independently. The proposed family of functions can be used to compare and refine multiscale measures of time series asymmetry. © 2010 Wiley Periodicals, Inc. *Complexity* 00: 000–000, 2010

Key Words: multiscale time asymmetry; irreversibility; arrow of time; sawtooth function; Weierstrass function; multiscale analysis of time series

Corresponding author: Anton Burykin, Emory Center for Critical Care (ECCC) and Department of Surgery, Emory University School of Medicine, Atlanta, GA;
e-mail: anton.burykin@emory.edu
URL: www.burykin.com

I. INTRODUCTION

Time irreversibility (asymmetry with respect to time reversal) is an important property of many observed time series. Such asymmetry is evidence of the nonlinearity of a time series, as linear Gaussian processes are time reversible [1]. Several statistical tests have been

developed toward detection and quantification of irreversibility in time series (see e.g., [2, 3]). The irreversibility of natural processes reflects the “arrow of time” and is a fundamental property of nonequilibrium systems [4]. Many complex time series (e.g., heart rate) demonstrate an even more complex, multiscale irreversibility such that not only the original but also coarse-grained time series are asymmetric within a range of scales. Several quantitative measures (indices) of multiscale irreversibility have been developed [5–10]. However, the relationships among these indices have not been studied, and it is possible that each of them measures a different aspect of multiscale time asymmetry. Besides their theoretical importance, such indices have practical applications. For example, indices of heart rate and electroencephalogram (EEG) time asymmetry (both single and multiscale) can be used as diagnostic tools (see e.g., [5–7, 11–18]).

Thus, it is important to investigate the properties of these indices of time asymmetry.¹ Note, that experimental and observational time series are not very suitable for such an analysis, since for example, they may contain other (both known and possibly unknown) types of “complexity,” which may affect the results of the asymmetry analysis and comparison of different asymmetry measures. Thus, there is a need to develop a simple deterministic time series with exactly known properties and variable multiscale asymmetry.

In this article, we introduce an asymmetric Weierstrass function W_A (constructed from asymmetric sawtooth functions instead of cosine waves) that can be used to construct time series with any prescribed value of the multiscale asymmetry. The article is organized as follows. In Section II, we define the multiscale asymmetry index [5,6] used in this study. In Section III, we define the classical and asymmetric Weierstrass functions and in Section IV, we calculate their multiscale asymmetry indices. We summarize and conclude in Section V.

II. DEFINITION OF MULTISCALE ASYMMETRY

To calculate the asymmetry index, an original time series $x(n)$, $n = 1, \dots, N$ (where N is the number of points in the time series) is transformed into a new time series of coarse-grained differences (for every scale $s = 1, \dots, S_{\max} \ll N$) defined as:

$$y_s(k) = x(k+s) - x(k) \quad k = 1, \dots, N-s \quad (1)$$

Individual terms (increments and decrements) in each new time series Eq. (1) quantify transitions between two

¹In this initial study, we consider only one index [5,6] of multiscale asymmetry. Theoretical analysis of other indices can be found, e.g., in [7, 8].

values in the original time series: an increase (activation) or a decrease (relaxation). For a perfectly symmetric time series, the number of increments is equal to the number of decrements. Thus, the time asymmetry can be defined at every scale s as a difference between the percentages (probabilities) of increments and decrements [6]:

$$Ai(s) = P^+(s) - P^-(s) = \frac{\sum_{k=1}^{N-s} \theta[-y_s(k)]}{N-s} - \frac{\sum_{k=1}^{N-s} \theta[y_s(k)]}{N-s} \quad (2)$$

Here, θ is the Heaviside function.

III. WEIERSTRASS AND ASYMMETRIC WEIERSTRASS FUNCTIONS

The Weierstrass function is the first published [19] example of a continuous but nowhere differentiable function. It is defined as follows:

$$W(t) = \sum_{k=1}^{K_{\max}} f_{\min}^{-kH} \cos(2\pi f_{\min}^k t) \quad (3)$$

Here, f_{\min} is the minimum frequency of oscillations and H is the so-called Hurst (or scaling) exponent ($0 < H < 1$), which is related to the fractal dimension, D , according to the following formula:

$$D = 2 - H \quad (4)$$

The power spectrum of the Weierstrass function has a “power law” shape

$$S(f) \sim 1/f^\beta \quad (5)$$

where the power exponent β is related to the Hurst exponent according to the relationship:

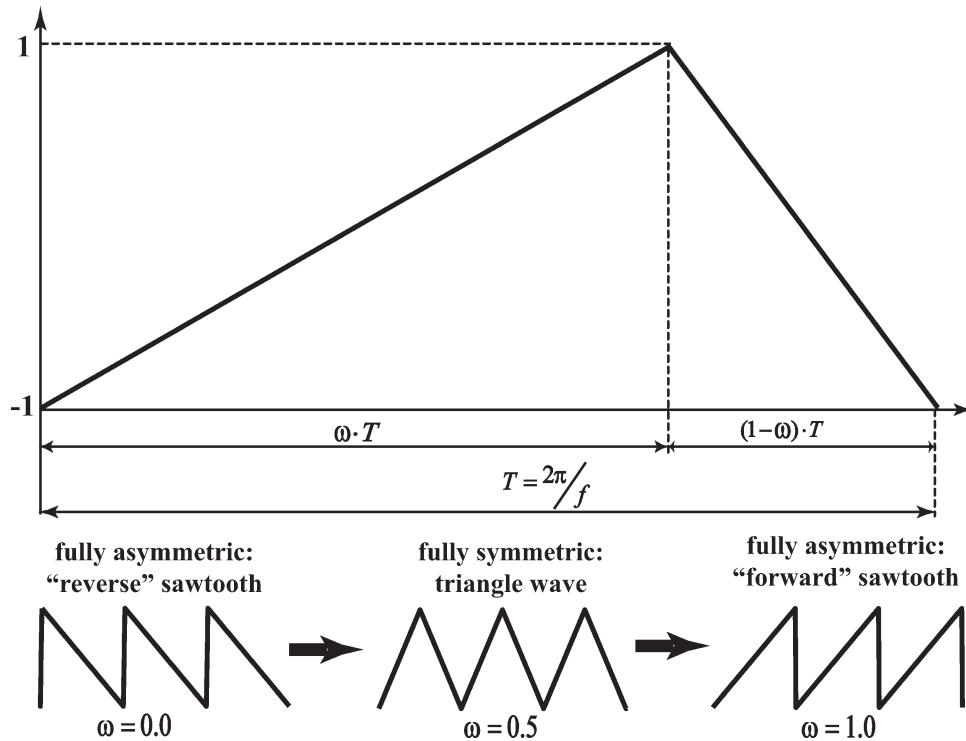
$$\beta = 2H + 1 \quad (6)$$

Note, that the detrended fluctuation analysis (DFA, [20]) exponent α is related to the Hurst exponent as:

$$H = \alpha - 1 \quad (7)$$

The Weierstrass function is also a classic model of a (multi) fractal process, and it is widely used in physics

FIGURE 1



Top: One period of the sawtooth function St (T and f are, correspondingly, the period and the frequency of the function). The asymmetry parameter ω ($0 \leq \omega \leq 1$) determines the relative position of the maximum within one period of the sawtooth function. Bottom: Three specific versions of the sawtooth function that correspond to the following values of the asymmetry parameter ω : $\omega = 0.0$ (fully asymmetric 'reverse' sawtooth), $\omega = 0.5$ (fully symmetric triangle wave) and $\omega = 1.0$ (fully asymmetric 'forward' sawtooth). Note that the functions that correspond to the two limiting cases ($\omega = 1$ and $\omega = 0$) are discontinuous.

and physiology (see e.g., [21–23]). However, the Weierstrass function is a sum of cosine waves and, therefore, reversible (time symmetric) at any mode (frequency) because the cosine function is symmetric with respect to time reversal operation. Thus, it cannot be used to model irreversible time series [with the irreversibility defined according to Eq. (2)].

To overcome this restriction, we introduce a modified Weierstrass function (the “asymmetric Weierstrass” function or W_A function) by substituting the cosine functions with sawtooth functions:

$$W_A(t) = \sum_{k=1}^{K_{\max}} f_{\min}^{-kH} St(2\pi f_{\min}^k t; \omega) \quad (8)$$

Here, ω ($0 \leq \omega \leq 1$) is the asymmetry parameter that determines the relative position of the maximum within one period of the sawtooth function $St(t)$ (in this study, we

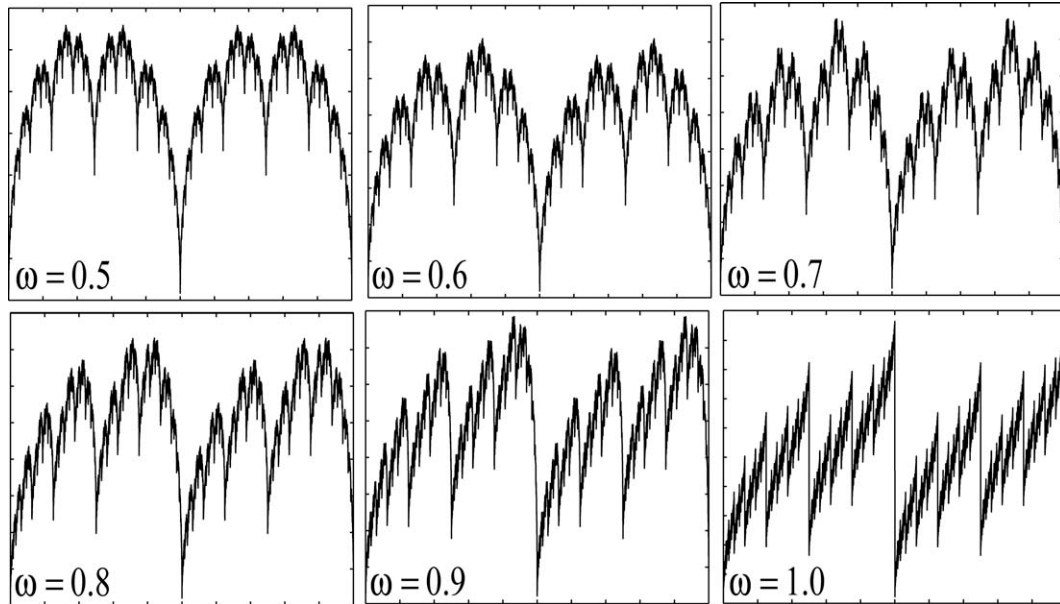
used the sawtooth function available in MATLAB [24]), see Figure 1. The asymmetric Weierstrass function Eq. (8) is deterministic and defined with a simple formula, so it is suitable for both theoretical analysis and numerical experiments.

The asymmetric Weierstrass function is irreversible at any mode (frequency). By varying the asymmetry parameter ω , we can continuously change the multiscale time asymmetry of the signal (Figure 2). Note that the W_A function constructed from fully symmetric ($\omega = 0.5$) sawtooth functions is equivalent to the “positive midpoint displacements” method of fractal time series construction (see e.g., [25]) and is a version of the Takagi function, another continuous but nowhere differentiable function [26].

IV. MULTISCALE ASYMMETRY OF THE W_A FUNCTION

To assess the dependence of the multiscale asymmetry index on the asymmetry parameter ω , we generated 101 W_A functions [Eq. (8)] with linearly increasing the asym-

FIGURE 2



Asymmetric Weierstrass function Eq. (8) with Hurst exponent $H = 0.5$ (corresponds to the classical Brownian motion), minimum frequency $f_{\min} = 2.0$ Hz and asymmetry parameter, ω varying from $\omega = 0.5$ (fully symmetric) to $\omega = 1.0$ (fully asymmetric).

metry parameter $\omega(n) = (n-1)/100$ ($n = 1, \dots, 101$) and Hurst exponent $H = 0.5$ (corresponds to regular Brownian motion). The length of each dataset was equal to $T_{\max} = 100$ s, and the sampling frequency was equal to $f_s = 5000$ Hz (therefore the each dataset had $N = 5 \cdot 10^5$ points). The maximum number of modes, K_{\max} , in Eq. (8) can be estimated from the Nyquist sampling theorem [27]: $f_{\max} \approx f_{\text{Nyquist}} = \frac{f_s}{2}$. Since $f_{\max} = f_{\min}^{K_{\max}}$ then $K_{\max} = \frac{\log(f_{\max})}{\log(f_{\min})} \approx \frac{\log(f_s/2)}{\log(f_{\min})}$. For the parameters used in this study ($f_s = 5000$ Hz, $f_{\min} = 1.5$ Hz), the lower bound is $K_{\max} \approx 20$. However, as $MsAi$ is a time-domain measure, we used a much larger value, $K_{\max} = 100$.

In Figure 3, we plot percentages of increments (P^+) and decrements (P^-) and their difference [Ai , see Eq. (2)], up to the scale $S_{\max} = 5000$ for the W_A function constructed from fully asymmetric ($\omega = 0.0$) sawtooth functions. Note that $N = 10^2 S_{\max}$, and thus, the condition $S_{\max} \ll N$ is satisfied.

There is no unique way to quantify multiscale asymmetry of a signal with a single number. Here, we employed one of many possible definitions. We observed that even for a “fully-asymmetric” ($\omega = 0.0$) W_A function, the asymmetry index Ai crosses zero at some scale S^* . Thus, we chose the sum of the asymmetry values up to the scale S^* (normalized by the value of that scale, S^*) as a quantitative measure of the signal multiscale asymmetry:²

$$MsAi = \frac{1}{S^*} \sum_{s=1}^{S^*} Ai(s) \quad (9)$$

where $Ai(s)$ is the asymmetry index at scale s , and S^* is the scale when the $Ai(s)$ crosses zero (changes the sign) for the first time.³ The $MsAi$ index depends monotonically (approximately linearly) on the asymmetry parameter ω (Figure 4). Thus, we can construct (by varying the asymmetry parameter ω) a time series with any prescribed (given) value of the multiscale asymmetry. This is the main result of the paper.

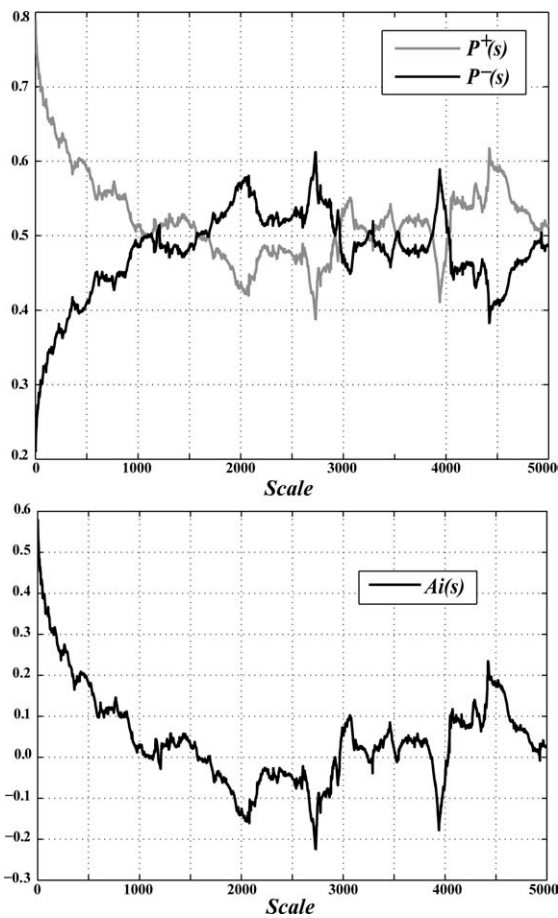
Note, that multiscale asymmetry is a property of a self-similar time series that is independent from its fractal dimension D (or, equivalently, its Hurst exponent). Indeed, it has been shown (see e.g., [28] and references, therein) that any function of the form

$$F(t) = \sum_{k=0}^{\infty} f^{-kH} g(f^k \cdot t) \quad (10)$$

²Two other possible definitions are area under the $Ai(s)$ curve (AUC) and a parameter from (e.g., exponential) fit of the $Ai(s)$ curve decay.

³Note, that the scale S^* depends on the sampling frequency f_s , but both the time constant $\tau = S^*/f_s$ (characteristic time of asymmetry) and the (normalized) asymmetry index $MsAi$ Eq. (9) are approximately constant for a wide range of the sampling frequencies. Thus, it would be an advantage to plot the asymmetry index versus characteristic frequency or characteristic time, instead of the scale.

FIGURE 3



Top: Percentages of increments (P^+) and decrements (P^-) and (bottom) asymmetry index Ai Eq. (2) as functions of scale s (up to the maximum scale $S_{\max} = 5000$) for the W_A function Eq. (8) constructed using fully asymmetric ($\omega = 0.0$) sawtooth functions.

where $g(t)$ is a periodic function that satisfies the Lipchitz-Holder condition of order H

$$|g(t + \Delta t) - g(t)| \leq C|\Delta t|^H \quad (11)$$

has scaling (Hurst) exponent H and fractal dimension $D = 2 - H$ (see also “Lipchitz-Holder heuristics” in [21]). As any sawtooth function is periodic and satisfies the condition defined by Eq. (11) for any value of the asymmetry parameter $\omega \in (0,1)$, the asymmetric Weierstrass function Eq. (8) has the same fractal dimension D regardless of the value of ω . In two limiting cases, $\omega = 0$ and $\omega = 1$, the corresponding sawtooth functions are discontinuous, and thus, they do not satisfy the Lipchitz-Holder condition.

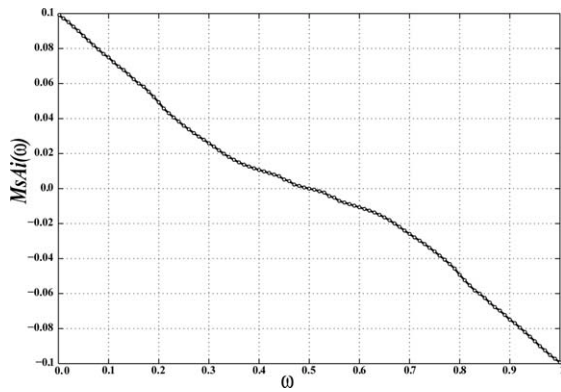
We also tested this statement numerically, by calculating the DFA exponent of our datasets. We calculated DFA-based Hurst exponents Eq. (7) from 101 W_A functions Eq. (8) with linearly increasing asymmetry parameter $\omega(n) = (n-1)/100$ ($n = 1, \dots, 101$) and Hurst exponent $H = 0.5$ (see Figure 5, top). The DFA-based Hurst exponent of the W_A function in the fully symmetric case ($\omega = 0.5$) becomes approximately equal to the DFA-based Hurst exponent of cosine-based W function (marked as “X” in Figure 5, top): $H_{\text{DFA}}(W_A; \omega = 0.5) = 0.4587$ and $H_{\text{DFA}}(W) = 0.4624$. Calculated DFA-based exponents of all asymmetric ($\omega \neq 0.5$) W_A functions are smaller than those of the symmetric W_A (or W) function. Again, as the theory predicts, this deviation becomes significant at the regions close to the two limiting cases, $\omega = 0$ and $\omega = 1$, where the Lipchitz-Holder condition is not valid. However, within a wide range of $\omega(0.2 \leq \omega \leq 0.8)$ the Hurst exponent is relatively independent from the asymmetry parameter, in agreement with the theory.⁴

Besides fractal dimension, multiscale asymmetry appears to be independent of some other multiscale complexity indices. As another numerical test, we computed multiscale entropies (MsEn) [29] of both cosine-based W function and 101 W_A functions with varying asymmetry parameter (again, in all the cases $H = 0.5$). The results demonstrate that for all values of ω , MsEn curves lie very close to each other (Figure 5, bottom). Again, we found that MsEn of the symmetric ($\omega = 0.5$) W_A function is practically indistinguishable from MsEn of the corresponding W function, whereas MsEn of fully asymmetric ($\omega = 0.0$ and $\omega = 1.0$) W_A functions are outliers at small scales.

Thus, $MsAi$ is independent (within a wide range of asymmetry parameter values) from other multiscale measures. The asymmetry parameter can be varied continu-

⁴As shown in Figure 5, all DFA-based exponents lie below the “theoretical” value ($H = 0.5$). We found that our DFA calculations systematically underestimate values of Hurst exponent Eq. (7) as compared with “theoretical” Hurst exponents used to construct W functions [both for cosine-based W Eq. (2) and W_A functions Eq. (8)]. This may be due to a finite number of modes (K_{\max}) in Eqs. (2) and (8) or because the summation started with $k = 1$ (not with $k = -K_{\max}$), so these functions are not truly “scale free.” Anyway, a detailed analysis of why the DFA method underestimates values of the Hurst exponents W -type functions is outside the scope of the article. Our goal was to demonstrate, via numerical calculations [in addition to the formal analysis, Eq. (11)], that the fractal dimension of the W_A function (measured by DFA exponent) remains approximately constant (regardless of the specific value of this constant) within a wide range of asymmetry parameter. Underestimation leads to a “systematic error,” which is nevertheless the same for all the datasets.

FIGURE 4



Multiscale asymmetry index MsAi Eq. (9) as a function of the asymmetry parameter ω for 101 W_A functions ($H = 0.5$, $f_{\min} = 1.5$ Hz).

ously (to construct a time series with any prescribed value of multiscale asymmetry) while preserving other multiscale properties. More detailed analysis is needed to determine the origin of the weak dependence of other multiscale properties (e.g., scaling exponent and multiscale entropy) from the asymmetry parameter ω around two limiting cases ($\omega = 0.0$ and $\omega = 1.0$).

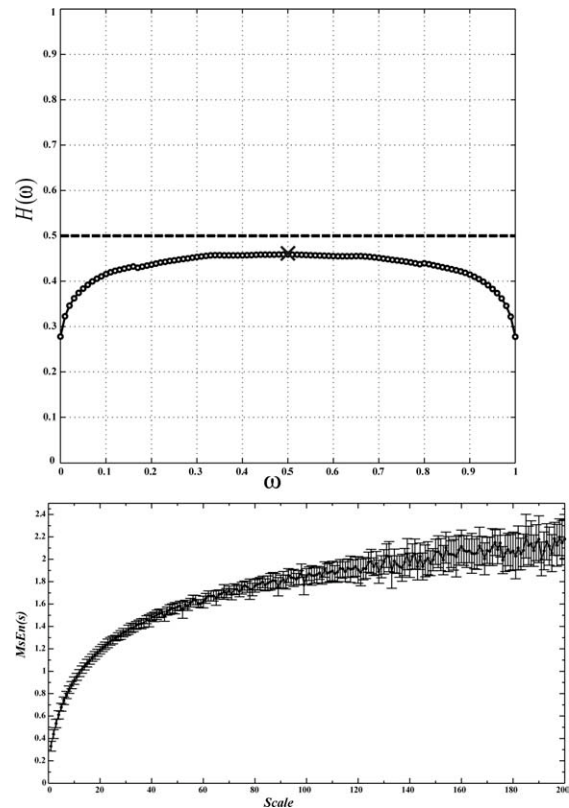
The proposed modification of the Weierstrass function permits one important generalization. Note, that if the Hurst exponent is time dependent, $H = H(t)$ (a time varying scaling exponent is usually referred as Holder exponent [30]), the Weierstrass function demonstrates multifractal properties [31, 32]. In a similar manner, we can introduce time-dependent (local) multiscale time asymmetry (irreversibility) $\omega = \omega(t)$. Such time dependent asymmetry may exist, for example in long-term (e.g., Holter monitor) recordings [33] of the heart rate, as its time asymmetry may depend on the level of physical activity (rest vs. intensive exercise or sleep vs. wake).⁵ An example of time-dependent (piecewise constant) multiscale time asymmetry is given below (where T is the length of time series), see Figure 6:

$$\omega(t) = \begin{cases} 0 & 0 \leq t < T/3 \\ 0.5 & T/3 \leq t < 2T/3 \\ 1 & 2T/3 \leq t < T \end{cases} \quad (12)$$

In this extreme case, multiscale time asymmetry has opposite signs in two parts of the time series. While multiscale

⁵Note that multiscale time asymmetry of heart rate time series can have different absolute values but always has the same sign.

FIGURE 5



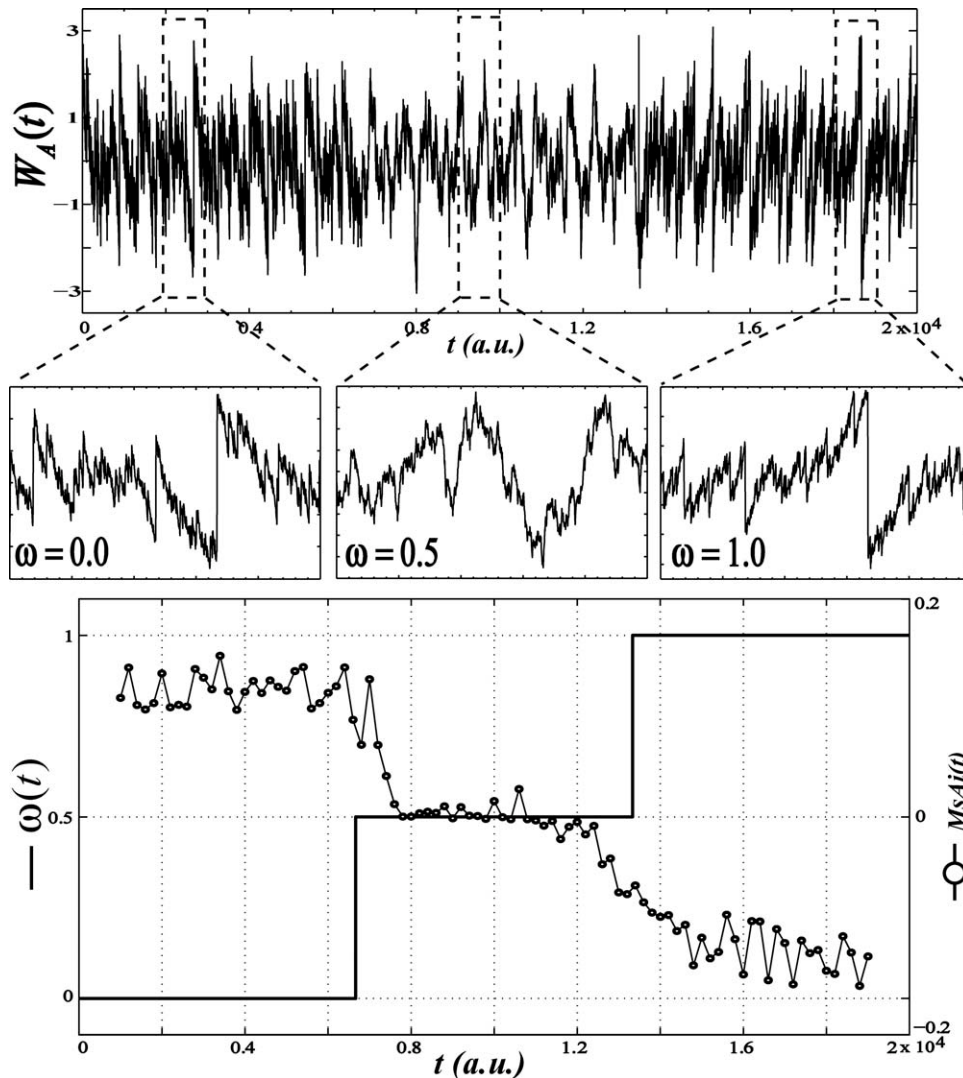
Multiscale complexity measures for 101 W_A functions Eq. (8) with different values of asymmetry parameter ω and the same Hurst exponent $H = 0.5$. Top: DFA-based Hurst exponents (—○—) and ‘theoretical’ Hurst exponent (---). The value of DFA-based Hurst exponent of cosine-based W function with Hurst exponent $H = 0.5$ is marked by ‘X’; (bottom) multiscale entropy (mean and standard deviation values vs. scale).

asymmetry of whole time series is zero, it is possible to recover such a time-dependent multiscale time asymmetry by dividing the initial time series into overlapping windows and applying the same algorithm [Eqs. (2) and (9)] to each window (Figure 6, bottom).

V. DISCUSSION

In this article, we introduced a new method of constructing a simple deterministic function (asymmetric Weierstrass function, W_A) with any prescribed value of multiscale asymmetry (irreversibility). Then, we provided evidence (both analytical and computational) that multiscale asymmetry index is independent of other multiscale complexity measures of time series (such as MsEn or DFA

FIGURE 6



Top: W_A Time series constructed using the asymmetry parameter ω defined by Eq. (12). (insets: fragments of the time series that have constant asymmetry parameter ω). Bottom: Piecewise constant asymmetry parameter ω Eq. (12) and time dependent multiscale asymmetry index $MsAi$, calculated using overlapping windows (window length is equal to 10% of the dataset length) with 90% overlap.

exponent). Finally, we generalized the concept of the multiscale asymmetry by introducing time-dependent (local) multiscale asymmetry and constructed examples of such time series. Thus, the W_A function combines two essential features of complex time series (e.g., healthy heart rate), namely fractality (multiscale self-similarity or long-range correlations) and irreversibility (multiscale time asymmetry); moreover, each of these features can be tuned independently.

Here, we have considered only the simplest case, where all modes in W_A function have the same value of the asymmetry parameter ω . Possible generalizations can include, for example, scale (mode)-dependent time asymmetry $\omega(k) = (k/K_{\max}) - 1$, so that the asymmetry is different for each mode (for every basis function) or $\omega = rand(1, K_{\max})$ (the asymmetry of every mode is chosen randomly). In general, the asymmetry parameter can depend on both time and mode, $\omega = \omega(k, t)$. Thus, a large

variety of test signals can be created to test different aspects of proposed asymmetry indices.

Interestingly, most of the classical continuous but nowhere differentiable (fractal or self-similar) functions are symmetric even on a single scale (for a historical review, see [34]). Also, the Takagi function is not the only fractal (continuous but nowhere differentiable) function constructed using the symmetric sawtooth function. Other examples include McCarthy [35] and Knopp [36] functions. Thus, multiscale asymmetric functions (with any prescribed degree of asymmetry) can be constructed from these functions as well.

Note, that the “power law” frequency dependence (logarithmic scale) in the Weierstrass function is somewhat inconvenient for numerical analysis, because both multiscale entropy MsEn and multiscale asymmetry MsAi use linear scales. Similarly, the Fourier transform [27] (in contrast to, e.g., Wavelet [37] or Constant-Q [38] transforms), which is used for calculation of scaling exponent from power spectrum, employs a linear sequence of frequencies. A simple example of multiscale asymmetric function (which we refer to as multiscale sawtooth function, *MsSt*) with linear sequence of frequencies is given below:

$$MsSt(t) = \sum_{k=1}^{K_{\max}} St(2\pi f_k t; \omega) \quad (13)$$

Here, *St* is a periodic sawtooth function with a frequency $f_k = f_{\max}/k$, $k = 1, \dots, K_{\max}$. Thus, the signal generated by Eq. (13) is time-asymmetric for every frequency component (mode) from $f_{\min} = f_{\max}/K_{\max}$ to f_{\max} . Multiscale properties (those discussed in this article) of *MsSt* function

⁶As the amplitude of all the modes in the Eq. (13) is constant, formally *MsSt* does not converge (in contrast to the Weierstrass function). However, the convergence property is only important when the number of modes is infinite (and in our case K_{\max} is finite).

⁷We should emphasize that the W_A function itself is not a “model” of any specific physiologic time series (such as heart rate), and thus is not intended to reproduce or mimic any particular property of such time series. Rather, it is a tool (a test function) to study properties of different multiscale asymmetry indices (which in turn are used to characterize physiologic time series). What we study in this article is not “physiologic time series,” but “complexity measures” (specifically, multiscale asymmetry index) used to characterize physiologic time series.

are similar to those of the W_A function.⁶ Namely, by varying the asymmetry parameter ω , we can continuously change the multiscale time asymmetry of the *MsSt* function. Other multiscale measures (DFA and MsEn) of the *MsSt* function are also independent from its asymmetry parameter (except around two limiting cases $\omega = 0.0$ and $\omega = 1.0$). It is also possible to construct piecewise nonlinear multiscale asymmetric functions of the forms Eqs. (8) or (13). One example is a multiscale asymmetric function constructed from repeated exponents instead of the linear functions used in the sawtooth function.

The applications of the proposed asymmetric Weierstrass function are not limited to physiological signals.⁷ For example, W_A -type signal is very similar to the multiscale fluctuations of temperature during long-term climate change [39] and fluctuations of TCP flow dynamics in communication networks (see e.g., [40, 41]). Note that a modified version (“piecewise-linear analog”) of the Weierstrass function constructed from fully asymmetric ($\omega = 0.0$) sawtooth functions with logarithmically decreasing frequencies (which is somewhat similar to both W_A and *MsSt* functions introduced in this article) was used to construct a deterministic model of Burgers turbulence [42]. We note possible applications of the W_A function as a model of rough surfaces (see e.g., [43, 44]) and of fractally asymmetric ratchet potentials (see e.g., [45, 46]).

Further, formal analysis is required to analytically derive the properties of the asymmetric Weierstrass function and to understand the behavior of multiscale asymmetry index. Specifically, the (in)dependence of *MsAi* from fractal dimension (and other “complexity measures”) has to be studied rigorously. It is interesting to investigate possible connections between W_A functions and so-called “asymmetric fractals” introduced in [47]. Finally, we need to reemphasize that all the results of this article were obtained by using only one specific definition (*MsAi* index [5, 6]) of multiscale asymmetry. One should calculate other indices of multiscale asymmetry [7–9] for the W_A function to systematically compare the results and clarify whether different indices capture different aspects of multiscale asymmetry.

Acknowledgments

This work was generously supported by grants from the DARPA (49533-LS-DRP, HR0011-05-1-0057, and FA9550-08-1-0364), the NIH (1 K99 AG030677-01A2 and U01EB008577), the James S. McDonnell Foundation, the Ellison Medical Foundation, and the Mathers Charitable Foundation.

References

1. Weiss, G. Time-reversibility of linear stochastic processes. *J Appl Probab* 1975, 12, 831–836.
2. Diks, C.; Vanhouwelingen, J.C.; Takens, F.; Degoede, J. Reversibility as a criterion for discriminating time-series. *Phys Lett A* 1995, 201, 221–228.
3. Stone, L.; Landan, G.; May, R.M. Detecting time's arrow: A method for identifying nonlinearity and deterministic chaos in time-series data. *Proc R Soc London Ser B: Biol Sci* 1996, 263, 1509–1513.
4. Prigogine, I.; Antoniou, I. Laws of nature and time symmetry breaking. *Tempos in Sci Nat: Struct, Relat, Complexity* 1999, 879, 8–28.
5. Costa, M.; Goldberger, A.L.; Peng, C.K. Broken asymmetry of the human heartbeat: Loss of time irreversibility in aging and disease. *Phys Rev Lett* 2005, 95, 198102–198104.
6. Costa, M.D.; Peng, C.K.; Goldberger, A.L. Multiscale analysis of heart rate dynamics: Entropy and time irreversibility measures. *Cardiovasc Eng* 2008, 8, 88–93.
7. Casali, K.R.; Casali, A.G.; Montano, N.; Irigoyen, M.C.; Macagnan, F.; Guzzetti, S.; Porta, A. Multiple testing strategy for the detection of temporal irreversibility in stationary time series. *Phys Rev E* 2008, 77, 066204–066207.
8. Porporato, A.; Rigby, J.R.; Daly, E. Irreversibility and fluctuation theorem in stationary time series. *Phys Rev Lett* 2007, 98, 094101–094104.
9. Alvarez-Ramirez, J.; Rodriguez, E.; Carlos Echeverria, J. A DFA approach for assessing asymmetric correlations. *Phys A: Stat Mech Appl* 2009, 388, 2263–2270.
10. Hou, F.Z.; Zhuang, J.J.; Bian, C.H.; Tong, T.J.; Chen, Y.; Yin, J.; Qiu, X.J.; Ning, X.B. Analysis of heartbeat asymmetry based on multi-scale time irreversibility test. *Phys A: Stat Mech Appl* 2010, 389, 754–760.
11. Porta, A.; Casali, K.R.; Casali, A.G.; Gnecci-Ruscione, T.; Tobaldini, E.; Montano, N.; Lange, S.; Geue, D.; Cysarz, D.; Van Leeuwen, P. Temporal asymmetries of short-term heart period variability are linked to autonomic regulation. *Am J Physiol Regul Integr Comp Physiol* 2008, 295, R550–R557.
12. Cammarota, C.; Rogora, E. Time reversal, symbolic series and irreversibility of human heartbeat. *Chaos, Solitons & Fractals* 2007, 32, 1649–1654.
13. van der Heyden, M.J.; Diks, C.; Pijn, J.P.M.; Velis, D.N. Time reversibility of intracranial human EEG recordings in mesial temporal lobe epilepsy. *Phys Lett A* 1996, 216, 283–288.
14. Ehlers, C.L.; Havstad, J.; Prichard, D.; Theiler, J. Low doses of ethanol reduce evidence for nonlinear structure in brain activity. *J Neurosci* 1998, 18, 7474–7486.
15. Edwards, R.; Beuter, A. Using time domain characteristics to discriminate physiologic and Parkinsonian tremors. *J Clin Neurophysiol* 2000, 17, 87–100.
16. Timmer, J.; Gantert, C.; Deuschl, G.; Honerkamp, J. Characteristics of hand tremor time-series. *Biol Cybern* 1993, 70, 75–80.
17. Porta, A.; Guzzetti, S.; Montano, N.; Gnecci-Ruscione, T.; Furlan, R.; Malliani, A. Time reversibility in short-term heart period variability. *Comput Cardiol* 2006, 2006, 77–80.
18. Porta, A.; D'addio, G.; Bassani, T.; Maestri, R.; Pinna, G.D. Assessment of cardiovascular regulation through irreversibility analysis of heart period variability: A 24 hours Holter study in healthy and chronic heart failure populations. *Phil Trans Math Phys Eng Sci* 2009, 36792, 1359–1375.
19. Weierstrass, K. On continuous functions of a real argument that do not have a well-defined differential quotient (1872). In: *Classics on Fractals*; Edgar, G.A. Ed; Reading, MA: Addison-Wesley, 1993; pp 2–9.
20. Peng, C.K.; Buldyrev, S.V.; Havlin, S.; Simons, M.; Stanley, H.E.; Goldberger, A.L. Mosaic organization of DNA nucleotides. *Phys Rev E* 1994, 49, 1685–1689.
21. Mandelbrot, B.B. *The Fractal Geometry of Nature*; Springer-Verlag: New York, 1982.
22. Bassingthwaite, J.B.; Liebovitch, L.S.; West, B.J. *Fractal physiology*. Oxford University Press: New York, 1994.
23. West, B.J.; Bologna, M.; Grigolini, P. *Physics of Fractal Operators*; Springer-Verlag: New York, 2003.
24. Little, J.; Shure, L. *Signal Processing Toolbox for Use with Matlab. User's Guide*; Mathworks: Natick, MA, 1992.
25. Peitgen, H.-O.; Saupe, D., Eds. *The Science of Fractal Images*; Springer-Verlag: New York, 1988; p 312.
26. Takagi, T. A simple example of a continuous function without derivative. *Proc Phys Math Jpn* 1903, 1, 176–177.
27. Blackledge, J.M.; Turner, M. *Digital Signal Processing: Mathematical and Computational Methods, Software Development and Applications*. Chichester: Horwood Publishing, 2003.
28. Hunt, B.R. The Hausdorff dimension of graphs of Weierstrass functions. *Proc Am Math Soc* 1998, 126, 791–800.
29. Costa, M.; Goldberger, A.L.; Peng, C.K. Multiscale entropy analysis of complex physiologic time series. *Phys Rev Lett* 2002, 89, 068102–068104.
30. Falconer, K. *Fractal Geometry: Mathematical Foundation and Applications*. Chichester: Wiley, 2003.
31. Daoudi, K.; Vehel, J.L.; Meyer, Y. Construction of continuous functions with prescribed local regularity. *Constr Approx* 1998, 14, 349–385.
32. Loutridis, S.J. An algorithm for the characterization of time-series based on local regularity. *Phys A: Stat Mech Appl* 2007, 381, 383–398.
33. Holter, N.J. New Method for Heart Studies: Continuous electrocardiography of active subjects over long periods is now practical. *Science* 1961, 134, 1214–1220.
34. Thim, J. *Continuous Nowhere Differentiable Functions (MS Thesis)*. Lulea: Lulea University of Technology, 2003.
35. McCarthy, J. An everywhere continuous nowhere differentiable function. *Am Math Mon* 1953, 60, 709.
36. Knopp, K. Ein einfaches Verfahren zur Bildung stetiger nirgends differenzierbarer Funktionen. *Math Z* 1918, 6, 118–123.
37. Addison, P.S. *The Illustrated Wavelet Transform Handbook*. London: Institute of Physics, 2002.

38. Brown, J.C. Calculation of a Constant-Q Spectral Transform. *J Acoust Soc Am* 1991, 89, 425–434.
39. Rial, J.A. Abrupt climate change: Chaos and order at orbital and millennial scales. *Global Planet Change*, 2004, 41, 95–109.
40. Kocarev, L.; Vattay, G., Eds. *Complex Dynamics in Communication Networks. Understanding Complex Systems*; Springer: Berlin, 2005.
41. Baccelli, F; Hong, D. Flow level simulation of large IP networks. Presented at INFOCOM 2003, 22nd Annual Joint Conference of the IEEE Computer and Communications Societies; San Francisco, CA: IEEE 2003.
42. Gurbatov, S.N.; Trussov, A.V. The decay of multiscale signals—a deterministic model of Burgers turbulence. *Phys D: Nonlinear Phenom* 2000, 145, 47–64.
43. He, L.; Zhu, J. The fractal character of processed metal surfaces. *Wear* 1997, 208, 17–24.
44. Lhernould, M.S.; Delchambre, A.; Regnier, S.; Lambert, P. Electrostatic forces in micromanipulations: Review of analytical models and simulations including roughness. *Appl Surf Sci* 2007, 253, 6203–6210.
45. Marchesoni, F. Transport properties in disordered ratchet potentials. *Phys Rev E* 1997, 56, 2492.
46. Mondal, D.; Ghosh, P.K.; Ray, D.S. Noise-induced transport in a rough ratchet potential. *J Chem Phys* 2009, 130, 074703–074707.
47. Doerer, D.M.; Sabharwal, C.L. A new twist to fractals. In: *Proceedings of the 17th conference on ACM Annual Computer Science Conference*; ACM: Louisville, Kentucky, 1989; pp 145–155.